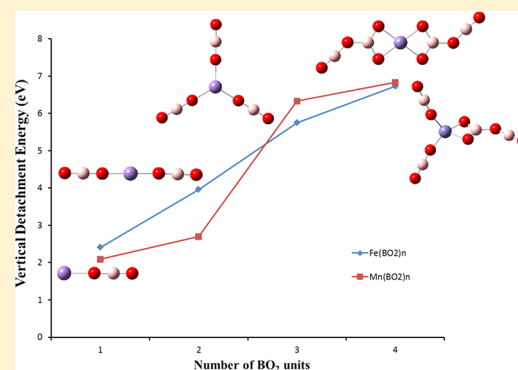


# Electronic and Magnetic Properties of Manganese and Iron Atoms Decorated With $\text{BO}_2$ Superhalogens

Pratik Koirala,<sup>†,||</sup> Kalpataru Pradhan,<sup>‡</sup> Anil K. Kandalam,<sup>\*,§</sup> and P. Jena<sup>\*,‡</sup><sup>†</sup>Department of Physics, McNeese State University, Lake Charles, Louisiana 70609, United States<sup>‡</sup>Department of Physics, Virginia Commonwealth University, Richmond, Virginia 23284, United States<sup>§</sup>Department of Physics, West Chester University, West Chester, Pennsylvania 19383, United States

**ABSTRACT:** Using density functional theory based calculations, we have systematically studied the equilibrium geometries, relative stabilities, and electronic and magnetic properties of Fe and Mn atoms interacting with a varying number of  $\text{BO}_2$  moieties. These clusters are found to exhibit hyperhalogen behavior with electron affinities as high as 6.9 eV once the number of  $\text{BO}_2$  moieties exceed the nominal valences of these transition metal atoms, namely 2 for both Fe and Mn. In all cases the transition metal atoms retain a sizable spin magnetic moment, even exceeding their free atom values at certain compositions. We also note that when more than two  $\text{BO}_2$  moieties are bound to neutral Fe and Mn atoms, they tend to dimerize. In the case of negative ions, this process occurs at  $n \geq 3$ , thus leading to different neutral and anionic ground state geometries. The effect of these structural changes in the interpretation of photoelectron spectroscopy experiments is discussed.



## I. INTRODUCTION

Negative ions play an important role in materials chemistry as strong oxidizing agents<sup>1</sup> and building blocks of energetic materials.<sup>2</sup> The halogen atoms, due to their  $ns^2 np^5$  outer electronic configuration, readily form negative ions and hence are an integral part of salts. Chlorine has the highest electron affinity,<sup>3,4</sup> namely 3.62 eV, of any element in the periodic table. Nearly half a century ago Bartlett and co-workers<sup>5,6</sup> discovered that a  $\text{PtF}_6$  molecule could oxidize Xe and estimated its electron affinity to be 6.8 eV. Later, Boldyrev and Gutsev coined the word *superhalogen*<sup>7</sup> to describe molecules like  $\text{PtF}_6$  that have electron affinities higher than that of Cl. They further showed that molecules that consist of a metal atom at the center and surrounded by halogen atoms all behave as superhalogens as long as the number of halogen atoms exceed the maximal valence of the metal atom by one.<sup>8,9</sup> Over the last 30 years, numerous works<sup>10–21</sup> have been published in this field showing the existence of superhalogens made of simple metal atoms such as alkali metal, Mg, and Al atoms at the core and halogen atoms such as F and Cl on the outside. The work on superhalogen moieties has been further extended to include coinage metal atoms<sup>22,23</sup> and transition metal atoms at the core.<sup>24–31</sup> Transition metals have the added advantage that they possess multiple valences and thus can exhibit superhalogen behavior for a varied number of halogen atoms. In addition, because transition metal atoms carry a magnetic moment, superhalogens containing these atoms can be magnetic.

Recently, it has been shown that it is not necessary for a superhalogen to consist of either a metal atom or halogen atom. For example,  $\text{BO}_2$  is a superhalogen<sup>32</sup> with an electron affinity

of 4.46 eV. Similarly, borane derivatives, such as  $\text{B}_n\text{H}_{n+1}$ ,  $\text{CB}_{n-1}\text{H}_n$ , and  $\text{MB}_n\text{H}_n$  ( $M = \text{alkali atom}, n > 4$ ) exhibit superhalogen behavior.<sup>33</sup> It is also possible to form superhalogens by replacing halogens with pseudohalogen moieties such as CN.<sup>34</sup> These possibilities have extended the field of superhalogens and literally hundreds of molecules can be designed to have rather large electron affinities. In another important development, it was discovered<sup>35</sup> that a new class of highly electronegative species can be formed if a metal atom is surrounded by superhalogens instead of halogens. Such species, when its electron affinity is larger than its superhalogen building blocks, are termed as *hyperhalogens*.<sup>35</sup> Hence, this provides a recipe for designing and synthesizing new molecules with very large electron affinities. The discovery of hyperhalogens first made in  $\text{Au}(\text{BO}_2)_n$  systems<sup>35</sup> has since been extended to  $\text{Cu}(\text{BO}_2)_n$  clusters,<sup>36</sup> simple metal atom (Na, Mg, and Al) containing borates<sup>37,38</sup> and  $\text{Na}(\text{BF}_4)_2$  systems.<sup>39</sup>

In this paper we focus on  $\text{Fe}(\text{BO}_2)_n$  and  $\text{Mn}(\text{BO}_2)_n$  ( $n = 1–4$ ) clusters. Although both Mn and Fe are transition metal elements, their magnetic properties are very different. Mn, with a  $3d^5 4s^2$  electronic configuration, exhibits a wide range of oxidation states ranging from 0 to +7; +2 being its most predominant oxidation state. Mn atoms possess a spin magnetic moment of  $5 \mu_B/\text{atom}$  and couple antiferromagnetically in the

**Special Issue:** Peter B. Armentrout Festschrift

**Received:** July 27, 2012

**Revised:** October 21, 2012

**Published:** November 1, 2012



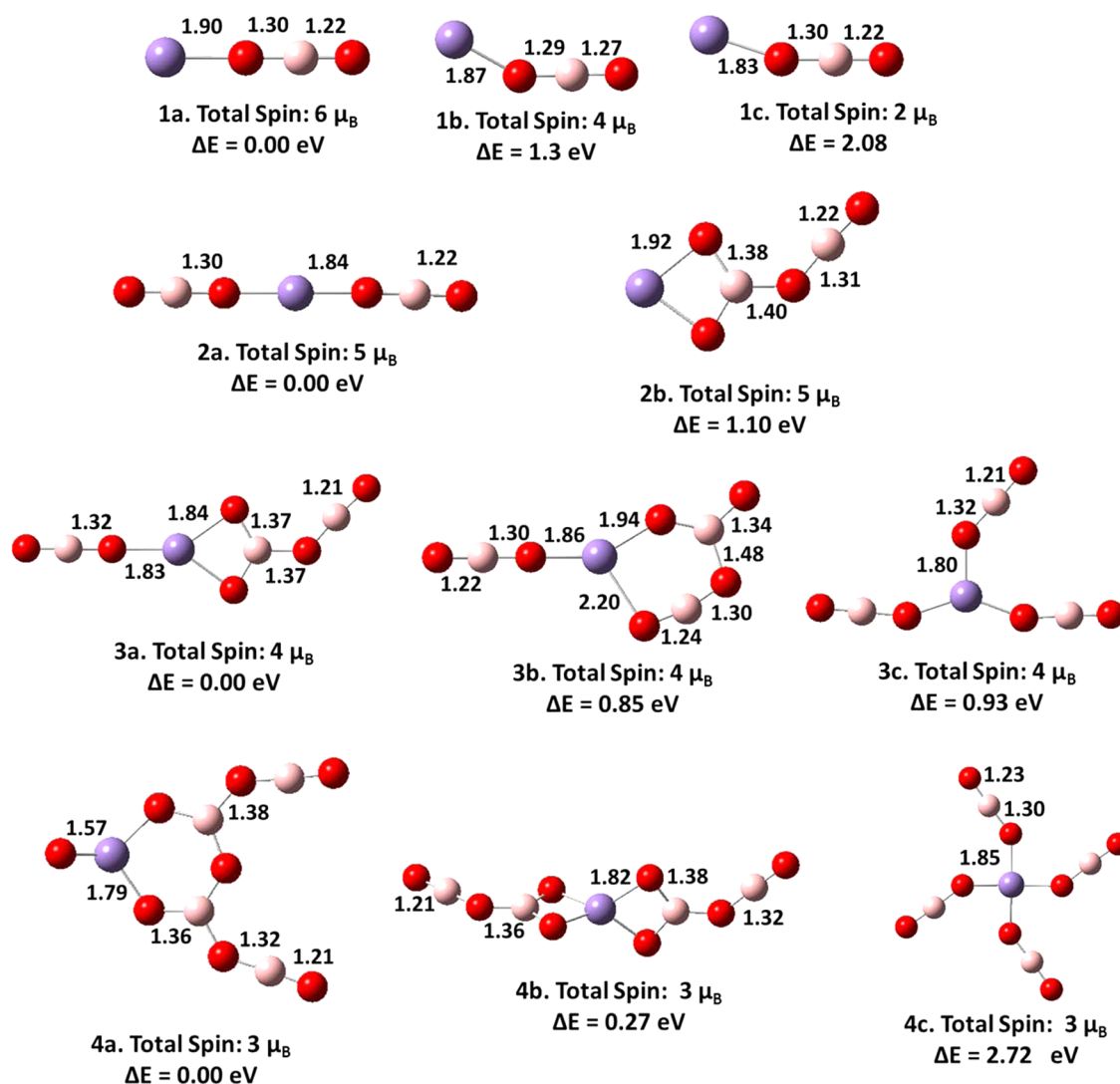


**Figure 1.** Lowest energy and higher energy isomers of neutral  $\text{Mn}(\text{BO}_2)_n$  ( $n = 1-4$ ) clusters. The total spin magnetic moments (in  $\mu_B$ ) along with the relative energies ( $\Delta E$  in eV) are also shown. All the bond lengths are given in Å.

bulk. Fe atoms, on the other hand, have predominant oxidation states of +2 and +3. With an electronic configuration of  $3d^6 4s^2$ , they carry a spin magnetic moment of  $4 \mu_B/\text{atom}$  and couple ferromagnetically in the bulk. It will be, thus, interesting to see if the above  $\text{TM}(\text{BO}_2)_n$  clusters exhibit hyperhalogen behavior and if so at what value of  $n$  does this property emerge? Equally important is to see if the metal atoms continue to carry a magnetic moment and if so do their values decrease with ligand decoration or can they be enhanced?

## II. COMPUTATIONAL DETAILS

Density functional theory based electronic structure calculations were carried out to determine the ground state geometries and the corresponding ground spin states of neutral and charged  $\text{TM}(\text{BO}_2)_n$  ( $\text{TM} = \text{Mn}$  and  $\text{Fe}$ ;  $n = 1-4$ ) clusters. The hybrid gradient corrected exchange–correlation functional<sup>40,41</sup> (B3LYP) in conjunction with 6-311+G(d) basis set as implemented in Gaussian 03 code,<sup>42</sup> was used for all the calculations. The reliability of our computational parameters was established in a previous study<sup>43</sup> on  $\text{Fe}_n(\text{BO}_2)_n$  clusters. In the geometry optimization procedure, the structural parameters of various isomers were fully optimized for several possible spin

states without any symmetry restrictions. Convergence criteria for total energies and forces were set to  $10^{-9}$  hartree, and  $10^{-4}$  hartree/Å, respectively. Furthermore, vibrational frequency calculations were also carried out to confirm the dynamic stability of these isomers.

We have calculated adiabatic detachment energies (ADE) and vertical detachment energies (VDE) values to determine the hyperhalogen behavior of these clusters. The ADE value was obtained by calculating the energy difference between the ground state geometry of the anionic cluster and the structurally similar isomer of its neutral counterpart. Similarly, vertical detachment energies (VDE) are calculated as the difference in energies between the anion and the neutral both at the anion's ground state geometry. In cases where the ground state geometries of neutral and anionic clusters are similar, the ADE of the anionic cluster is equal to the electron affinity (EA) of the corresponding neutral cluster. The analysis that follows is from the perspective of anionic lowest energy structure and its structurally similar neutral cluster, because photoelectron spectroscopy is a vertical process where the neutral cluster, following the electron detachment, may not have enough time to reach its ground state if it is protected by a large energy barrier.

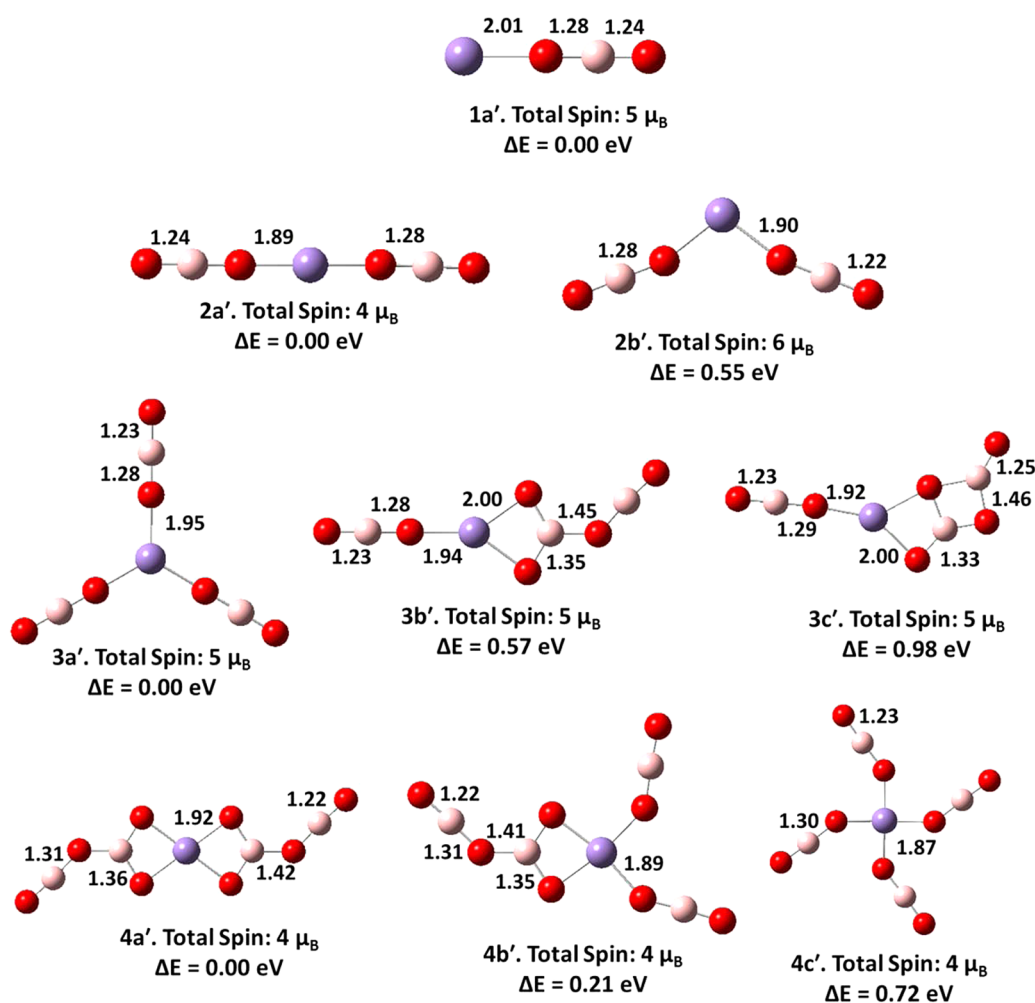


**Figure 2.** Lowest energy and higher energy isomers of negatively charged  $\text{Mn}(\text{BO}_2)_n$  ( $n = 1-4$ ) clusters. The total spin magnetic moments (in  $\mu_B$ ) along with the relative energies ( $\Delta E$  in eV) are also shown. All the bond lengths are given in Å.

### III. RESULTS AND DISCUSSION

First, we will discuss our results on neutral and anionic  $\text{Mn}(\text{BO}_2)_n$  followed by discussions of  $\text{Fe}(\text{BO}_2)_n$  clusters.

**A.  $\text{Mn}(\text{BO}_2)_n$  ( $n = 1-4$ ) Clusters.** The ground state and higher energy isomers of neutral and anionic  $\text{Mn}(\text{BO}_2)_n$  clusters along with their spin magnetic moments are given in Figures 1 and 2, respectively. Our calculated VDE, ADE, and the NBO charges on the Mn atom in the ground state anion and its corresponding neutral cluster are given in Table 1. The ground state of both the neutral and anionic  $\text{Mn}(\text{BO}_2)_n$  clusters is found to be a linear structure, with the metal atom binding to one of the oxygen atoms of the  $\text{BO}_2$  unit. The Mn–O bond

**Table 1.** Vertical Detachment Energies (VDE) and Adiabatic Detachment Energies (ADE) of Negatively Charged  $\text{Mn}(\text{BO}_2)_n$  ( $n = 1-4$ ) Clusters<sup>a</sup>

cluster	isomer	VDE (eV)	ADE (eV)	charge on Mn ( <i>e</i> )	
				neutral	anion
$[\text{Mn}(\text{BO}_2)]^-$	1a'	2.09	1.99	0.89	-0.02
$[\text{Mn}(\text{BO}_2)_2]^-$	2a'	2.70	2.59	1.61	0.70
$[\text{Mn}(\text{BO}_2)_3]^-$	3a'	6.33	5.71	1.80	1.66
$[\text{Mn}(\text{BO}_2)_4]^-$	4a'	6.83	6.28	1.67	1.66

<sup>a</sup>The NBO charges on the metal atom are also listed.

length in the neutral cluster (Figure 1, 1a) is 1.90 Å, whereas in the case of the anion (Figure 2, 1a'), the bond length increased to 2.01 Å. The most preferred spin multiplicity, ( $M = 2S + 1$ ) of the neutral  $\text{Mn}(\text{BO}_2)$  cluster is a septet, leading to the spin magnetic moment of  $6 \mu_B$ , whereas in the case of the anionic cluster the preferred spin magnetic moment is  $5 \mu_B$ . The nature of bonding between the Mn atom and the  $\text{BO}_2$  unit in the  $\text{Mn}(\text{BO}_2)$  cluster is ionic in nature, with a net NBO charge of  $+0.90e$  on Mn atom (Table 1) and  $-0.90e$  on the  $\text{BO}_2$  moiety. The calculated values of VDE and ADE for  $[\text{Mn}(\text{BO}_2)]^-$  are 2.09 and 1.99 eV, respectively. Because the ground state structures of neutral and anionic clusters are identical, the ADE of the anion corresponds to the EA of the neutral  $\text{Mn}(\text{BO}_2)$  cluster. As expected, the EA value of  $\text{Mn}(\text{BO}_2)$  is significantly larger than the EA values of  $\text{MnX}$  ( $X = \text{F}, \text{Cl}, \text{and Br}$ ) cluster. For example, the EA of  $\text{MnF}$ ,  $\text{MnCl}$ , and  $\text{MnBr}$  are reported<sup>31</sup> to be 1.34, 1.52, and 1.59 eV, respectively, whereas the EA of  $\text{Mn}(\text{BO}_2)$  is 1.99 eV. Another isomer, in which the cluster forms a bent structure is significantly higher in energy for both neutral (Figure 1, 1b) and anionic (Figure 2, 1b') cases.

In the case of the  $\text{Mn}(\text{BO}_2)_2$  cluster, the two  $\text{BO}_2$  moieties can bind to the Mn atom as separate units, as reported in the  $\text{Au}(\text{BO}_2)_2$  cluster,<sup>35</sup> or they can dimerize to form the  $\text{B}_2\text{O}_4$  moiety and then interact with the Mn atom as a single unit. We have taken both these scenarios into account during the

geometry optimization. The ground state geometries of both neutral and anionic  $\text{Mn}(\text{BO}_2)_2$  clusters correspond to a configuration, where each unit of  $\text{BO}_2$  is bonded to the Mn atom separately, thereby forming a linear structure (Figure 1, 2a, and Figure 2, 2a'). The spin multiplicity of neutral  $\text{Mn}(\text{BO}_2)_2$  is a sextet, resulting in a spin magnetic moment of  $5 \mu_B$ , with the majority of this moment localized on the Mn atom. The spin magnetic moment of the  $[\text{Mn}(\text{BO}_2)_2]^-$  cluster is  $4 \mu_B$ . The structural configuration containing a  $\text{B}_2\text{O}_4$  unit was found to be 1.10 eV higher in energy for the neutral cluster (Figure 1, 2b), whereas a bent configuration with two individual  $\text{BO}_2$  units was found to be 0.55 eV higher in energy for anionic cluster (Figure 2, 2b').

The NBO charge analysis of the neutral  $\text{Mn}(\text{BO}_2)_2$  cluster (Figure 1, 2a), revealed a charge transfer of almost two electrons from the Mn atom to the two  $\text{BO}_2$  moieties, with a charge of  $+1.6e$  on the Mn atom (Table 1) and a charge of  $-0.80e$  on each of the  $\text{BO}_2$  units, resulting in a strong ionic bond between the doubly charge central metal ion and two  $\text{BO}_2^-$  moieties. Therefore, the oxidation state of Mn in the  $\text{Mn}(\text{BO}_2)_2$  cluster is +2, which is consistent with the spin magnetic moment of  $5 \mu_B$  for this cluster. The  $\text{Mn}(\text{BO}_2)_2$  cluster is, thus, expected to be highly stable against dissociation into smaller clusters. This is indeed the case, which will be evident from our discussion of the thermodynamic stabilities of these clusters in the following section. Interestingly, in the case of the  $[\text{Mn}(\text{BO}_2)_2]^-$  cluster (Figure 2, 2a'), the charge on Mn is only  $+0.7e$ , indicating that when the extra electron is added to the  $\text{Mn}(\text{BO}_2)_2$  cluster, the majority of the extra electron's charge (90%) is localized over the positively charged Mn atom (Table 1). In the anion photoelectron spectroscopy (PES) experiments, it is the anionic cluster from which the electron is photodetached. Thus, if one tries to understand the above charge distribution from the experimental viewpoint, i.e., PES experiments of the  $[\text{Mn}(\text{BO}_2)_2]^-$  cluster, then it can be said that the photodetached electron comes from the positively charged Mn, which results in the neutral  $\text{Mn}(\text{BO}_2)_2$  cluster containing  $\text{Mn}^{2+}$  and two  $\text{BO}_2^-$  units. The calculated VDE and ADE values of  $[\text{Mn}(\text{BO}_2)_2]^-$  cluster are 2.70 and 2.59 eV, respectively. Because there is no significant change in the ground state geometries of neutral and anionic clusters, the EA of  $\text{Mn}(\text{BO}_2)_2$  is also 2.59 eV. Even though the addition of the second  $\text{BO}_2$  unit to the  $\text{Mn}(\text{BO}_2)$  cluster has resulted in an increase in the EA value by 0.6 eV (from 1.99 to 2.59 eV), it is not larger than that of the  $\text{BO}_2$  superhalogen moiety (4.32 eV). Hence,  $\text{Mn}(\text{BO}_2)_2$  is not a hyperhalogen. This is consistent with the fact that in  $\text{Mn}(\text{BO}_2)_2$ , the Mn atom is in its most preferred oxidation state of +2 and each of the  $\text{BO}_2$  units have their required one-electron, thus a relatively low EA. On the other hand, when the EA of  $\text{Mn}(\text{BO}_2)_2$  is compared with the corresponding EA values of  $\text{MnX}_2$  ( $X = \text{F}, \text{Cl}, \text{and Br}$ ) clusters, an interesting picture emerges. The previously reported<sup>31</sup> EA values of  $\text{MnF}_2$ ,  $\text{MnCl}_2$ , and  $\text{MnBr}_2$  clusters are 1.25, 1.10, and 1.76 eV, respectively, which are substantially smaller than that of the EA of  $\text{Mn}(\text{BO}_2)_2$  cluster. Thus, it is evident that as one replaces the halogen atoms around a central metal atom with the superhalogen moieties, one can significantly increase the EA of the resulting cluster. A similar scenario was also observed in  $\text{AuX}_2$  and  $\text{Au}(\text{BO}_2)_2$  clusters.<sup>35</sup>

On further increasing the number of  $\text{BO}_2$  units to three, we obtain different ground state geometries for neutral and anionic  $\text{Mn}(\text{BO}_2)_3$  cluster. The ground state geometry of  $[\text{Mn}(\text{BO}_2)_3]^-$  cluster corresponds to a planar, symmetric structure in which

each of the three  $\text{BO}_2$  moieties is bonded to the Mn atom separately (Figure 2, 3a'). The spin magnetic moment of  $[\text{Mn}(\text{BO}_2)_3]^-$  cluster is  $5 \mu_B$ , with the spin localized on the Mn atom. In this structure, thus, the Mn atom has a  $3d^5$  configuration and is in +2 oxidation state. The isomer in which two of the  $\text{BO}_2$  units dimerize, while the third  $\text{BO}_2$  moiety binds separately to the Mn atom (Figure 2, 3b'), was found to be 0.57 eV higher in energy than the ground state structure. This higher energy isomer, thus, can be viewed as  $\text{BO}_2\text{-Mn-B}_2\text{O}_4$ . Interestingly, in the case of neutral  $\text{Mn}(\text{BO}_2)_3$  cluster, this higher energy  $\text{BO}_2\text{-Mn-B}_2\text{O}_4$  structure is found to be the ground state structure (Figure 1, 3a), whereas the structure similar to the ground state anion was found to be 0.93 eV higher in energy (Figure 1, 3c). The  $\text{Mn}(\text{BO}_2)_3$  cluster has a spin magnetic moment of  $4 \mu_B$ . The ground state geometry of the anionic  $\text{Mn}(\text{BO}_2)_3$  cluster is similar to the previously reported<sup>37</sup>  $[\text{Mg}(\text{BO}_2)_3]^-$  cluster. These similarities in the  $[\text{Mg}(\text{BO}_2)_3]^-$  and  $[\text{Mn}(\text{BO}_2)_3]^-$  clusters can be understood from the fact that both Mg and Mn prefer to be in the +2 oxidation state, which is the case when all the  $\text{BO}_2$  molecules are bonded as separate units with the metal atom. The calculated values of VDE and ADE of the  $[\text{Mn}(\text{BO}_2)_3]^-$  cluster are 6.33 and 5.71 eV, respectively, which are significantly larger than the corresponding electron detachment energies of the  $[\text{Mn}(\text{BO}_2)_2]^-$  cluster. Because the ground state geometries of the neutral and anionic  $\text{Mn}(\text{BO}_2)_3$  cluster are different, the ADE does not correspond to the EA of the neutral cluster. The calculated EA of the  $\text{Mn}(\text{BO}_2)_3$  cluster is 4.78 eV. Because the EA of the  $\text{Mn}(\text{BO}_2)_3$  cluster is larger than that of  $\text{BO}_2$  and because the cluster is also magnetic, we classify  $\text{Mn}(\text{BO}_2)_3$  as a *magnetic hyperhalogen*. However, it is to be noted here that, in the anion PES experiments, the electron detachment from the ground state  $[\text{Mn}(\text{BO}_2)_3]^-$  cluster results in a neutral cluster (Figure 1, 3c) that is 0.93 eV higher in energy than the ground state neutral cluster. Therefore, in the PES spectra of the  $[\text{Mn}(\text{BO}_2)_3]^-$ , the threshold energy, which is the electron binding energy (EBE), would be equal to our calculated ADE value, but not to EA. On the basis of our calculations, we expect an unusually large EBE of 5.71 eV in the PES spectra of the  $[\text{Mn}(\text{BO}_2)_3]^-$  cluster, thereby classifying the resultant neutral cluster as a *magnetic hyperhalogen*. This large EBE is due to the fact that in the case of the anion, the detached electron is delocalized over the three  $\text{BO}_2$  moieties. The NBO charges (Table 1) also show that the charge on the metal atom does not change ( $\Delta Q = -0.14e$ ) significantly as we go from anion  $\text{Mn}(\text{BO}_2)_3$  to its corresponding neutral cluster, indicating that the extra electron is delocalized over the three  $\text{BO}_2$  moieties. This is in contrast to the charge distribution scenario observed in the  $\text{Mn}(\text{BO}_2)_2$  cluster, where the extra electron's charge was localized mostly on the Mn atom. The delocalization of the extra electron over the  $\text{BO}_2$  units combined with the  $3d^5$  configuration of Mn, result in the enhanced stability of  $[\text{Mn}(\text{BO}_2)_3]^-$  cluster and can appear as a high intense peak (magic cluster) in the mass spectrum of  $[\text{Mn}(\text{BO}_2)_n]^-$  clusters. A similar scenario was observed in  $\text{Mn}_x\text{Cl}_y^-$  clusters.<sup>30</sup> We look forward to experimental verification of these predictions. Following the trend observed in smaller clusters, the ADE values of  $(\text{MnX}_3)^-$  ( $X = \text{F}, \text{Cl}, \text{and Br}$ ) cluster, reported in an earlier study<sup>31</sup> ( $\text{MnF}_3$ , 3.42 eV;  $\text{MnCl}_3$ , 4.50 eV;  $\text{MnBr}_3$ , 4.58 eV), are significantly lower than the ADE (5.71 eV) of  $[\text{Mn}(\text{BO}_2)_3]^-$  cluster.

The ground state geometry of  $[\text{Mn}(\text{BO}_2)_4]^-$  cluster is composed of two y-shaped  $\text{B}_2\text{O}_4$  units bonded to the central

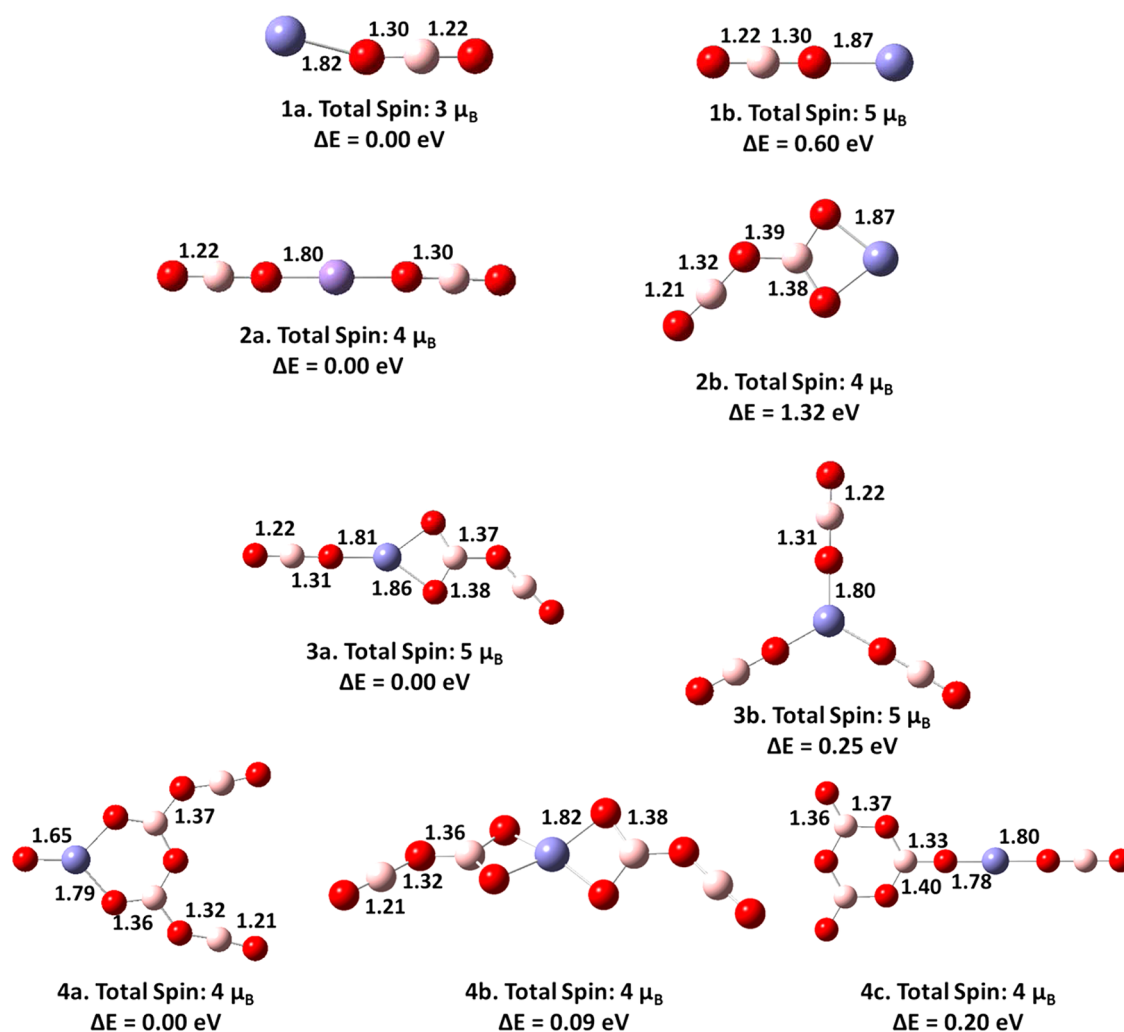


**Figure 3.** Lowest energy and higher energy isomers of neutral  $\text{Fe}(\text{BO}_2)_n$  ( $n = 1-4$ ) clusters. The total spin magnetic moments (in  $\mu_B$ ) along with the relative energies ( $\Delta E$  in eV) are also shown. All the bond lengths are given in Å.

Mn atom (Figure 2, 4a'), whereas the structure in which a  $\text{B}_2\text{O}_4$  unit and two  $\text{BO}_2$  moieties bind to the Mn atom (Figure 2, 4b') was found to be 0.21 eV higher in energy. Another structural configuration (Figure 2, 4c') in which all the four  $\text{BO}_2$  units bind to the Mn atom separately, thereby having a shape similar to an equilateral cross, was found to be 0.72 eV higher in energy. Note that, in all these structures the Mn atom is 4-fold coordinated and is in the +3 oxidation state. The  $[\text{Mn}(\text{BO}_2)_4]^-$  cluster prefers a quintet spin multiplicity and thus has a spin magnetic moment of  $4 \mu_B$ . As expected, the spin moment is completely localized over the manganese atom. The ground state geometry of the neutral  $\text{Mn}(\text{BO}_2)_4$  cluster (Figure 1, 4a) is not similar to its corresponding anion ground state geometry. The ground state structure of the neutral  $\text{Mn}(\text{BO}_2)_4$  cluster has a form where a  $\text{O}-\text{Mn}$  unit is bonded to a  $\text{B}_4\text{O}_7$  unit. However, a structural configuration that is similar to the ground state anion (Figure 1, 4b) is found to be just 0.27 eV higher in energy than the ground state neutral cluster, whereas the "equilateral-cross" structure (Figure 1, 4c) is 2.72 eV higher in energy. Note that in both the ground state (Figure 1, 4a) and the higher energy isomer (Figure 1, 4b), the Mn atom is in +4 oxidation state. The  $\text{Mn}(\text{BO}_2)_4$  cluster has a spin magnetic moment of  $3 \mu_B$ , which is consistent with the +4 state of Mn. The VDE and ADE for the ground state anion are 6.83 and

6.28 eV, respectively, whereas the EA of the neutral cluster is calculated to be 6.01 eV. Thus,  $\text{Mn}(\text{BO}_2)_4$  is also classified as a *magnetic hyperhalogen*. The NBO charge analysis of the anionic  $\text{Mn}(\text{BO}_2)_4$  cluster and its corresponding neutral cluster shows that the extra electron is completely delocalized over the two  $\text{B}_2\text{O}_4$  units, thus leading to a large electron binding energy.

Overall, we have shown that replacing the halogen atom X in the  $\text{MnX}_n$  cluster with a superhalogen moiety,  $\text{BO}_2$ , substantially enhances the electron affinity of the resulting cluster, with  $\text{Mn}(\text{BO}_2)_n$  ( $n = 3, 4$ ) clusters exhibiting hyperhalogen behavior. In negatively charged  $\text{Mn}(\text{BO}_2)_n$  clusters, as the number of  $\text{BO}_2$  moieties is increased, structures that maximize the delocalization of the extra electron and optimize the oxidation state of Mn atom are stabilized more than the structures containing  $\text{B}_2\text{O}_4$  units. On the other hand, in the case of neutral clusters with  $n > 2$ , structures containing  $\text{B}_2\text{O}_4$  and  $\text{B}_4\text{O}_7$  units dominate. Furthermore, the addition of  $\text{BO}_2$  moieties to the Mn atom decreases its spin magnetic moment from  $6 \mu_B$  in  $\text{Mn}(\text{BO}_2)$  to  $3 \mu_B$  in  $\text{Mn}(\text{BO}_2)_4$ .

**B.  $\text{Fe}(\text{BO}_2)_n$  ( $n = 1-4$ ) Clusters.** We now discuss the interaction of Fe atom with  $\text{BO}_2$  moieties. The ground state and higher energy structures of neutral and negatively charged  $\text{Fe}(\text{BO}_2)_n$  ( $n = 1-4$ ) clusters are shown in Figures 3 and 4, respectively. The calculated VDE, ADE, and the NBO charges

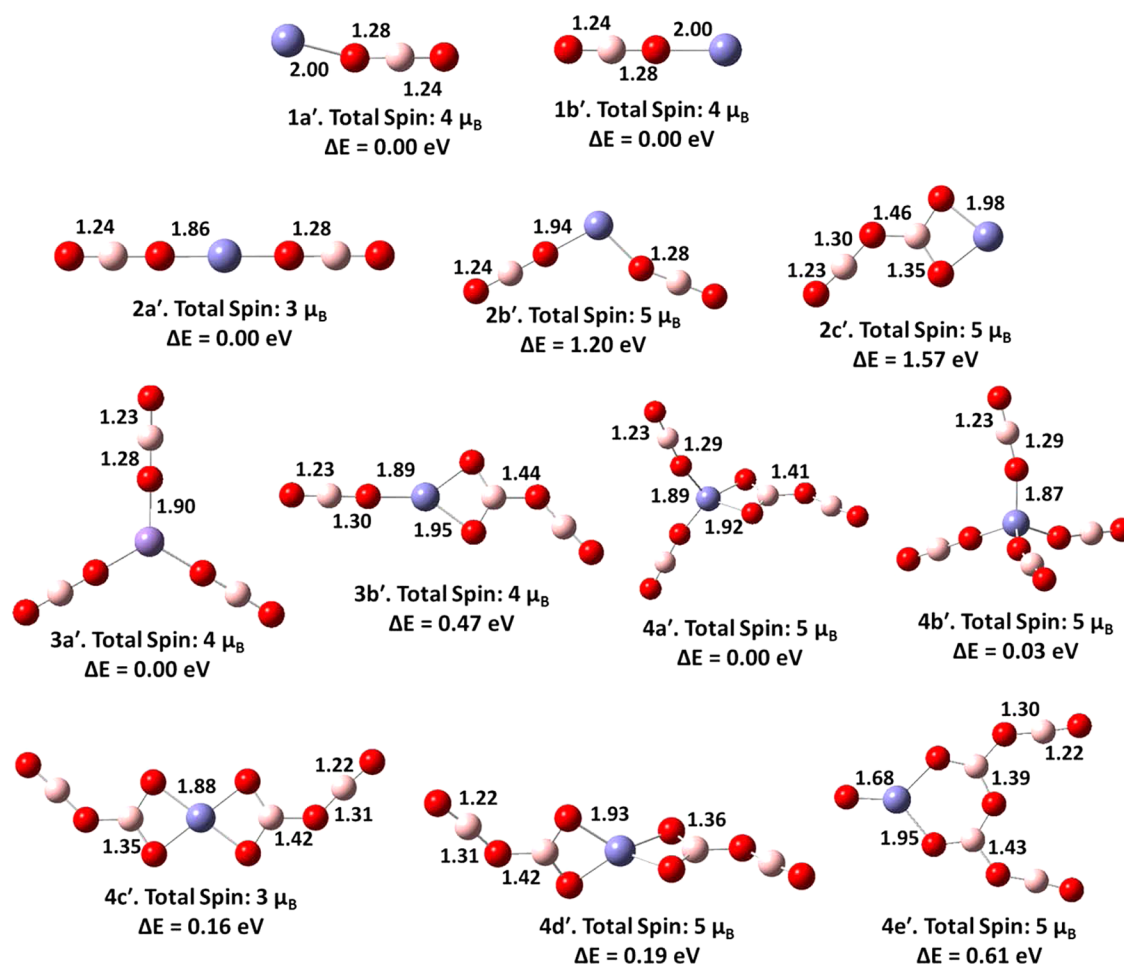


**Figure 4.** Lowest energy and higher energy isomers of negatively charged  $\text{Fe}(\text{BO}_2)_n$  ( $n = 1-4$ ) clusters. The total spin magnetic moments (in  $\mu_B$ ) along with the relative energies ( $\Delta E$  in eV) are also shown. All the bond lengths are given in Å.

on the Fe atom are given in Table 2. The neutral and anionic  $\text{Fe}(\text{BO}_2)_n$  ( $n = 1, 2$ ) clusters bear no major structural

**Table 2. Vertical Detachment Energies (VDE) and Adiabatic Detachment Energies (ADE) of Negatively Charged  $\text{Fe}(\text{BO}_2)_n$  ( $n = 1-4$ ) Clusters<sup>a</sup>**

cluster	isomer	VDE (eV)	ADE (eV)	charge on Fe (e)	
				neutral	anion
$[\text{Fe}(\text{BO}_2)]^-$	1a'	2.41	1.91	0.79	-0.02
$[\text{Fe}(\text{BO}_2)_2]^-$	2a'	3.96	3.80	1.48	0.76
$[\text{Fe}(\text{BO}_2)_3]^-$	3a'	5.75	5.73	1.93	1.55
	3b'	5.12	4.75	1.38	1.26
$[\text{Fe}(\text{BO}_2)_4]^-$	4a'	6.73	6.37	1.58	1.58
	4b'	7.21	6.89	1.89	1.88
	4c'	5.81	5.39	1.39	1.20

<sup>a</sup>The NBO charges on the metal atom are also listed.

differences apart from minor distortions due to the extra electron in the case of anions. The ground state geometries of both neutral and anionic  $\text{Fe}(\text{BO}_2)$  clusters is a bent structure. The neutral  $\text{Fe}(\text{BO}_2)$  cluster has a quartet spin multiplicity ( $2S + 1 = 4$ ), resulting in a spin magnetic moment of  $3 \mu_B$ . As expected, the spin moment is localized on the Fe atom. The nature of the bonding between the Fe atom and the  $\text{BO}_2$  unit is found to be ionic in nature, with a charge transfer of  $-0.79e$  from the Fe atom to the  $\text{BO}_2$  moiety. The most preferred spin

multiplicity of  $[\text{Fe}(\text{BO}_2)]^-$  cluster is a quintet, thus resulting in a spin magnetic moment of  $4 \mu_B$ . In the case of the anion, the majority of the extra electron's charge (77%) was found to be localized over the  $\text{BO}_2$  unit, and 23% of the charge goes to the positively charged Fe. Note that in the case of the  $[\text{Mn}(\text{BO}_2)]^-$  cluster, a larger portion (87%) of the extra electron's charge was localized on the  $\text{BO}_2$  moiety. This difference in the amount of localization is due to the fact that the iron atom has a larger electron affinity than the manganese atom. A linear isomer, similar to the ground state structure of the  $\text{Mn}(\text{BO}_2)$  cluster, was found to be 0.60 eV higher in energy (Figure 3, 1b) than the ground state structure of the  $\text{Fe}(\text{BO}_2)$  cluster, whereas in the case of the anion, this linear isomer is found to be energetically degenerate (Figure 4, 1b'). Our calculated VDE and ADE values of the  $[\text{Fe}(\text{BO}_2)]^-$  cluster are 2.41 and 1.91 eV, respectively (Table 2). These values are in good agreement with previously reported<sup>43</sup> experimental VDE and ADE values of 2.28 and 2.04 eV, respectively.

The lowest energy isomers of neutral and anionic  $\text{Fe}(\text{BO}_2)_2$  cluster adopt a linear structure with the two  $\text{BO}_2$  units binding to the metal atoms separately (Figure 3, 2a, and Figure 4, 2a'). The structure containing the  $\text{B}_2\text{O}_4$  unit binding to the Fe atom was found to be 1.32 eV higher in energy in the neutral (Figure 3, 2b), whereas in the case of the anion, it is 1.57 eV higher in energy (Figure 4, 2c'). Thus, the neutral and charged  $\text{Fe}(\text{BO}_2)_2$  clusters adopt similar structural features as the corresponding  $\text{Mn}(\text{BO}_2)_2$  cluster. The neutral  $\text{Fe}(\text{BO}_2)_2$  cluster prefers a spin

state (2S) of  $4 \mu_B$ , whereas its anionic counterpart has a spin magnetic moment of  $3 \mu_B$ . The calculated VDE and ADE values of the  $[\text{Fe}(\text{BO}_2)_2]^-$  cluster are 3.96 and 3.80 eV, respectively (Table 2). These electron detachment energies are not only larger than the  $[\text{Fe}(\text{BO}_2)]^-$  cluster (Table 2) but also about 1.2 eV larger than the corresponding energies of  $[\text{Mn}(\text{BO}_2)_2]^-$  cluster (Table 1). The larger electron detachment energies in the case of the  $[\text{Fe}(\text{BO}_2)_2]^-$  cluster is due to the fact that the extra electron is delocalized over the Fe (72%) and the two  $\text{BO}_2$  units (28%), whereas in the case of the  $[\text{Mn}(\text{BO}_2)_2]^-$  cluster, 90% of the extra electron's charge was localized over the Mn atom. This delocalization of the extra electron has caused a larger electron binding energy in the  $[\text{Fe}(\text{BO}_2)_2]^-$  as compared to the  $[\text{Mn}(\text{BO}_2)_2]^-$  cluster. The ADE of the anion, in this case, can be considered as the EA of the neutral  $\text{Fe}(\text{BO}_2)_2$  cluster. Because this EA is greater than 3.62 eV, the  $\text{Fe}(\text{BO}_2)_2$  cluster can be classified as a superhalogen. However, it still does not show hyperhalogen behavior because its EA is not larger than that of the  $\text{BO}_2$  (4.32 eV).

The lowest energy isomer of the neutral  $\text{Fe}(\text{BO}_2)_3$  cluster corresponds to a structure containing a *y-shaped*  $\text{B}_2\text{O}_4$  unit and a  $\text{BO}_2$  moiety binding to the Fe atom from either side (Figure 3, 3a). Note that the  $\text{Mn}(\text{BO}_2)_3$  cluster also has a similar structure. On the other hand, the structure in which all the three  $\text{BO}_2$  moieties are bonded to the Fe atom separately is 0.25 eV higher in energy (Figure 3, 3b). Note that in the case of the  $\text{Mn}(\text{BO}_2)_3$  cluster, the isomer containing three  $\text{BO}_2$  units (Figure 1, 3c) was found to be significantly higher in energy ( $\Delta E = 0.93$  eV) than its corresponding lowest energy structure. The stabilization of the isomer containing three separate  $\text{BO}_2$  units in the case of the  $\text{Fe}(\text{BO}_2)_3$  cluster can be due to the fact that in this isomer, the Fe atom is in the +3 oxidation state, its most preferred state. Both these isomers prefer a sextet spin multiplicity, leading to a spin magnetic moment of  $5 \mu_B$ . In the case of the negatively charged  $\text{Fe}(\text{BO}_2)_3$  cluster, however, the  $\text{BO}_2$  units prefer to bind separately to the Fe atom, leading to a planar structure (Figure 4, 3a'), whereas the geometry corresponding to the ground state neutral cluster is 0.47 eV higher in energy (Figure 4, 3b'). This reversal in the most preferred structures as one goes from neutral to anion was also observed in the  $\text{Mn}(\text{BO}_2)_3$  cluster. The  $[\text{Fe}(\text{BO}_2)_3]^-$  cluster has a spin magnetic moment of  $4 \mu_B$ . The NBO charge analysis of the anionic cluster and its corresponding neutral isomer showed that the majority of the extra electron's charge (62%) in the anion was delocalized over the three  $\text{BO}_2$  moieties and the charge on the Fe atom did not change ( $\Delta Q = -0.38e$ ) appreciably due to the electron detachment. Thus, the charge distribution in  $[\text{Fe}(\text{BO}_2)_3]^-$  is more delocalized than in the case of the  $[\text{Fe}(\text{BO}_2)_2]^-$  cluster. Therefore, we expect the ADE and VDE values of  $[\text{Fe}(\text{BO}_2)_3]^-$  to be substantially larger than the corresponding values of the  $[\text{Fe}(\text{BO}_2)_2]^-$  cluster. The VDE of  $[\text{Fe}(\text{BO}_2)_3]^-$  was calculated to be 5.75 eV, whereas the ADE is 5.73 eV (Table 2). The EA of the  $\text{Fe}(\text{BO}_2)_3$  cluster was found to be 5.48 eV. Because these electron-detachment energies are greater than the EA of  $\text{BO}_2$ , following the definition of hyperhalogens, we can also classify  $\text{Fe}(\text{BO}_2)_3$  cluster as a *magnetic hyperhalogen*.

On further increasing the number of  $\text{BO}_2$  units to four, several low lying isomers were found in both neutral and anionic  $\text{Fe}(\text{BO}_2)_4$  clusters. The lowest energy structure of the  $[\text{Fe}(\text{BO}_2)_4]^-$  cluster consists of a  $\text{B}_2\text{O}_4$  unit and two separate  $\text{BO}_2$  moieties bonded to the Fe atom (Figure 4, 4a'), with the plane of the  $\text{B}_2\text{O}_4$  unit perpendicular to rest of the cluster.

Interestingly, the structure in which all four  $\text{BO}_2$  units are separately bonded to the central Fe atom was found to be just 0.03 eV higher in energy (Figure 4, 4b'). Here again, a competition between the formation of  $\text{B}_2\text{O}_4$  units and achieving a larger delocalization to stabilize the metal–borate cluster is observed. In isomer 4b', the extra electron is delocalized over four  $\text{BO}_2$  units, whereas in the case of isomer 4a', the extra electron is delocalized over two  $\text{BO}_2$  units and a  $\text{B}_2\text{O}_4$  unit. The small difference in the NBO charges on the Fe atom of these two isomers (Table 2) clearly shows a slightly larger delocalization of electron in isomer 4b'. Both these isomers prefer a sextet spin multiplicity, leading to a spin magnetic moment of  $5 \mu_B$  for the  $[\text{Fe}(\text{BO}_2)_4]^-$  cluster. Note that neither of these two isomers was lower in energy in the case of the  $[\text{Mn}(\text{BO}_2)_4]^-$  cluster. The structural configuration containing two  $\text{B}_2\text{O}_4$  units binding to the Fe atom is 0.16 eV higher in energy (Figure 4, 4c'), whereas another conformation of the same structure (Figure 4, 4d') is 0.19 eV higher in energy than the lowest energy isomer. Unlike the two lowest energy structures, the isomers containing the  $\text{B}_2\text{O}_4$  units prefer a quartet spin multiplicity. The two lowest energy isomers of the neutral  $\text{Fe}(\text{BO}_2)_4$  cluster (Figure 3, 4a and 4b), on the other hand, are identical to the lowest energy structure of the  $\text{Mn}(\text{BO}_2)_4$  cluster (Figure 1, 4a and 4b). The lowest energy isomer (Figure 3, 4a), of  $\text{Fe}(\text{BO}_2)_4$  has a  $\text{B}_4\text{O}_7$  unit binding to a Fe–O unit. Another isomer, containing two  $\text{B}_2\text{O}_4$  units bound to the Fe atom (Figure 3, 4b) is only 0.09 eV higher in energy than the lowest energy isomer. The isomer corresponding to the anionic ground state was found to be 0.91 eV higher in energy, whereas the isomer containing four  $\text{BO}_2$  units is 1.45 eV higher in energy. The VDE and ADE values of the lowest energy isomer (Figure 4, 4a') are 6.73 and 6.37 eV, respectively (Table 2). The corresponding electron detachment energies of the next lower energy isomer (Figure 4, 4b') are substantially higher, with a VDE value of 7.21 eV and ADE of 6.89 eV (Table 2), which is a result of a larger delocalization of the extra electron over four  $\text{BO}_2$  units. Because the ADE value of the  $[\text{Fe}(\text{BO}_2)_4]^-$  cluster is greater than the EA/ADE of its superhalogen building unit,  $\text{BO}_2$ , and the cluster carries a large spin magnetic moment, it can be characterized as a *magnetic hyperhalogen*.

**C. Thermodynamic Stabilities.** The thermodynamic stabilities of the  $\text{TM}(\text{BO}_2)_n$  (TM = Mn, Fe;  $n = 1-4$ ) against fragmentation into smaller clusters were studied by considering various fragmentation paths and products. The fragmentation pathways and the corresponding dissociation energies for neutral and anionic clusters are given in Tables 3 and 4, respectively. The dissociation energies are all positive and hence these clusters are stable against fragmentation. The dissociation of  $\text{TM}(\text{BO}_2)_2$  into  $\text{TM}(\text{BO}_2) + \text{BO}_2$  fragments requires large energies of 4.58 and 4.00 eV for  $\text{Mn}(\text{BO}_2)_2$  and

**Table 3. Fragmentation Pathways and Dissociation Energies for Neutral  $\text{Mn}(\text{BO}_2)_n$  and  $\text{Fe}(\text{BO}_2)_n$  ( $n = 1-4$ ) Clusters**

cluster	pathways	dissociation energy (eV)	
		M = Mn	M = Fe
$\text{M}(\text{BO}_2)$	$\text{M} + \text{BO}_2$	3.68	3.72
$\text{M}(\text{BO}_2)_2$	$\text{M}(\text{BO}_2) + \text{BO}_2$	4.58	4.00
$\text{M}(\text{BO}_2)_3$	$\text{M}(\text{BO}_2)_2 + \text{BO}_2$	2.76	3.10
	$\text{M}(\text{BO}_2) + (\text{BO}_2)_2$	5.64	5.41
$\text{M}(\text{BO}_2)_4$	$\text{M}(\text{BO}_2)_3 + \text{BO}_2$	2.79	2.72

**Table 4. Fragmentation Pathways and Dissociation Energies for Anionic  $\text{Mn}(\text{BO}_2)_n$  and  $\text{Fe}(\text{BO}_2)_n$  ( $n = 1-4$ ) Clusters**

cluster	pathways	dissociation energy (eV)	
		M = Mn	M = Fe
$[\text{M}(\text{BO}_2)]^-$	$\text{M} + (\text{BO}_2)^-$	1.32	1.27
	$\text{M}^- + (\text{BO}_2)$	6.20	5.22
$[\text{M}(\text{BO}_2)_2]^-$	$[\text{M}(\text{BO}_2)]^- + \text{BO}_2$	5.18	5.89
	$\text{M}(\text{BO}_2) + (\text{BO}_2)^-$	2.82	3.44
$[\text{M}(\text{BO}_2)_3]^-$	$[\text{M}(\text{BO}_2)_2]^- + \text{BO}_2$	4.94	4.53
	$\text{M}(\text{BO}_2)_2 + (\text{BO}_2)^-$	3.18	3.97
$[\text{M}(\text{BO}_2)_4]^-$	$\text{M}(\text{BO}_2)_3 + (\text{BO}_2)^-$	3.60	3.83
	$[\text{M}(\text{BO}_2)_3]^- + \text{BO}_2$	3.18	2.95
	$\text{M}(\text{BO}_2)_2 + (\text{BO}_2)_2^-$	4.35	4.92
	$[\text{M}(\text{BO}_2)_2]^- + (\text{BO}_2)_2$	6.42	5.79

$\text{Fe}(\text{BO}_2)_2$ , respectively. For the  $\text{TM}(\text{BO}_2)_3$  cluster, we have considered two fragmentation paths: (i) one where the cluster fragments into  $\text{TM}(\text{BO}_2)_2$  and  $\text{BO}_2$  and (ii) the other where the cluster fragments into  $\text{TM}(\text{BO}_2)$  and  $(\text{BO}_2)_2$ , as illustrated in Table 3. The dissociation of  $\text{TM}(\text{BO}_2)_3$  into  $\text{TM}(\text{BO}_2)_2 + \text{BO}_2$  is preferred over dissociation into  $\text{TM}(\text{BO}_2) + (\text{BO}_2)_2$  in both  $\text{Mn}(\text{BO}_2)_3$  (by 2.88 eV) and  $\text{Fe}(\text{BO}_2)_3$  clusters (by 2.31 eV). The most preferred fragmentation pathway of  $\text{TM}(\text{BO}_2)_3$ , along with the large dissociation energy of the  $\text{TM}(\text{BO}_2)_2$  cluster, further establishes the stability of  $\text{TM}(\text{BO}_2)_2$  cluster, as discussed in the earlier section. Finally, in the case of the  $\text{TM}(\text{BO}_2)_4$  cluster, due to the complexity of the structure we considered only the fragmentation corresponding to the loss of one  $\text{BO}_2$  unit. The dissociation energy clearly shows that the cluster is stable against losing a  $\text{BO}_2$  unit.

In the case of negatively charged  $\text{TM}(\text{BO}_2)_n$  clusters, we have relatively more fragmentation pathways available due to the presence of the extra electron (Table 4). The competition between the fragmentation products in retaining the extra electron dictates the preferred fragmentation path. In the case of the  $[\text{TM}(\text{BO}_2)]^-$  ( $\text{TM} = \text{Mn}$  and  $\text{Fe}$ ) cluster, the dissociation leading to  $\text{TM} + \text{BO}_2^-$  is favored over dissociation into  $\text{TM}^- + \text{BO}_2$  by a significant amount of energy. This scenario is consistent with the electronic charge deficiency and the superhalogen characteristic of the  $\text{BO}_2$  moiety. In the case of the  $[\text{TM}(\text{BO}_2)_2]^-$  cluster, the most preferred fragmentation path corresponds to dissociation into  $\text{TM}(\text{BO}_2) + \text{BO}_2^-$ . The preference for the negative charge to reside on the  $\text{BO}_2$  unit during the fragmentation is again due to the fact that although  $\text{TM}(\text{BO}_2)$  is not a superhalogen in either Mn or Fe case, the  $\text{BO}_2$  is a superhalogen. This trend continues to the  $[\text{TM}(\text{BO}_2)_3]^-$  cluster as well, with the  $\text{TM}(\text{BO}_2)_2 + \text{BO}_2^-$  fragmentation path costing less energy than the  $[\text{TM}(\text{BO}_2)_2]^- + \text{BO}_2$  fragments. Interestingly, in the  $[\text{Fe}(\text{BO}_2)_3]^-$  cluster, the difference between the dissociation energies of the two fragmentation pathways is 0.56 eV, whereas in the case of the  $[\text{Mn}(\text{BO}_2)_3]^-$  cluster, this difference is significantly larger (1.76 eV). This is due to the fact that the neutral  $\text{Mn}(\text{BO}_2)_2$  is a highly stable species with a low electron affinity (2.59 eV), whereas in the case of iron,  $\text{Fe}(\text{BO}_2)_2$  is a superhalogen (EA: 3.80 eV), albeit not as strong as the  $\text{BO}_2$  unit (EA: 4.32 eV). Therefore, in the dissociation of the  $[\text{Fe}(\text{BO}_2)_3]^-$  cluster, there is a competition between the  $\text{Fe}(\text{BO}_2)_2$  and  $\text{BO}_2$  units in acquiring the negative charge, whereas in the case of  $[\text{Mn}(\text{BO}_2)_3]^-$ , there is no such competition. Only in the case of the  $[\text{TM}(\text{BO}_2)_4]^-$  cluster does the most favored fragmentation pathway result in a neutral  $\text{BO}_2$  unit and

negatively charged  $\text{TM}(\text{BO}_2)_3$  cluster. This change in the preferred fragmentation products is consistent with the fact that the EA value of  $\text{BO}_2$  is larger than that of  $\text{TM}(\text{BO}_2)$  and  $\text{TM}(\text{BO}_2)_2$  but less than that of the  $\text{TM}(\text{BO}_2)_3$  cluster.

#### IV. SUMMARY

In summary, we have carried out density functional theory based calculations to identify the equilibrium geometries and magnetic properties of  $\text{TM}(\text{BO}_2)_n$  ( $\text{TM} = \text{Mn}, \text{Fe}; n = 1-4$ ) clusters. We note that in neutral  $\text{Mn}(\text{BO}_2)_n$  clusters, the  $\text{BO}_2$  moieties bind individually for  $n = 1$  and 2 but begin to dimerize and polymerize for  $n = 3, 4$ . This is consistent with the fact that the predominant oxidation state of Mn is +2. In  $[\text{Mn}(\text{BO}_2)_n]^-$  clusters, the  $\text{BO}_2$  moieties continue to bind individually until  $n = 3$  and dimerize at  $n = 4$ . The spin magnetic moment of Mn atom in neutral  $\text{Mn}(\text{BO}_2)_n$  varies from  $6 \mu_B$  at  $n = 1-3$  to  $3 \mu_B$  at  $n = 4$ , decreasing by  $1 \mu_B$  with the addition of every  $\text{BO}_2$  moiety. In the anionic  $\text{Mn}(\text{BO}_2)_n$  cluster, on the other hand, the spin magnetic moment at the Mn atom is  $5 \mu_B$  for  $n = 1, 3$ , and  $4 \mu_B$  for  $n = 2, 4$ .  $\text{Mn}(\text{BO}_2)_3$  and  $\text{Mn}(\text{BO}_2)_4$  clusters, with adiabatic detachment energies of 5.71 and 6.28 eV, respectively are hyperhalogens, because these exceed the electron affinity of  $\text{BO}_2$  which is 4.46 eV.

In neutral  $\text{Fe}(\text{BO}_2)_n$  clusters, the  $\text{BO}_2$  moieties bind individually to the Fe atom until  $n = 2$ . They dimerize and polymerize respectively at  $n = 3$  and 4. This shows that the preferred oxidation number of Fe in these clusters is +2. The spin magnetic moments at the Fe atom site in  $\text{Fe}(\text{BO}_2)_n$  ( $n = 1-4$ ) clusters are respectively 3, 4, 5, and  $4 \mu_B$ . Note that the spin magnetic moment of a free Fe atom is  $4 \mu_B$ . Thus, it is possible for a transition metal atom ligated to  $\text{BO}_2$  to carry a spin moment that is larger than that of its neutral free atom. In the anionic  $\text{Fe}(\text{BO}_2)_n$  clusters,  $\text{BO}_2$  moieties bind individually until  $n = 3$ . With the adiabatic detachment energies of 5.73 eV for  $[\text{Fe}(\text{BO}_2)_3]^-$  and 6.37 eV for  $[\text{Fe}(\text{BO}_2)_4]^-$ , these clusters are hyperhalogens. Our results establish that Mn and Fe decorated with  $\text{BO}_2$  not only have hyperhalogen behavior but also carry a magnetic moment, irrespective of the number of  $\text{BO}_2$  moieties. Hence, these clusters can be termed as magnetic super- and hyperhalogens. We await experimental confirmation of our predictions.

#### ■ AUTHOR INFORMATION

##### Corresponding Author

\*E-mail: A.K., akandalam@wcupa.edu; P.J., pjena@vcu.edu.

##### Present Address

<sup>†</sup>Department of Materials Science and Engineering, Northwestern University, Evanston, IL 60208.

##### Notes

The authors declare no competing financial interest.

#### ■ ACKNOWLEDGMENTS

P.K. thanks Honors College of McNeese State University for providing partial financial support. P.J. acknowledges partial support from the U.S. Department of Energy and resources of the National Energy Research Scientific Computing Center, which is supported by the Office of Science of the U.S. Department of Energy under Contract No. DE-AC02-05CH11231.

## ■ REFERENCES

- (1) Hunt, D. F.; Stafford, G. C., Jr.; Crow, F. W.; Russell, J. W. *Anal. Chem.* **1976**, *48*, 2098–2104.
- (2) Bartlett, N.; Lucier, G.; Shen, C.; Casteel, W. J.; Chacon, L.; Munznerberg, J.; Zemva, B. *J. Fluorine Chem.* **1995**, *71*, 163–164.
- (3) Hotop, H.; Lineberger, W. C. *J. Phys. Chem. Ref. Data* **1985**, *14*, 731–750.
- (4) Berzins, U.; Gustafsson, M.; Hanstorp, D.; Klinkmuller, A.; Ljungblad, U.; Martenssonpendrill, A. M. *Phys. Rev. A* **1995**, *51*, 231–238.
- (5) Bartlett, N. *Proc. Chem. Soc.* **1962**, *6*, 218.
- (6) Bartlett, N.; Lohmann, D. H. *Proc. Chem. Soc.* **1962**, *3*, 115–116.
- (7) Gutsev, G. L.; Boldyrev, A. I. *Chem. Phys.* **1981**, *56*, 277–283.
- (8) Gutsev, G. L.; Boldyrev, A. I. *Chem. Phys. Lett.* **1984**, *108*, 250–254.
- (9) Scheller, M. K.; Compton, R. N.; Cederbaum, L. S. *Science* **1995**, *270*, 1160–1166.
- (10) Gutsev, G. L.; Boldyrev, A. I. *J. Phys. Chem.* **1990**, *94*, 2256–2259.
- (11) Boldyrev, A. I.; Simons, J. J. *Chem. Phys.* **1991**, *97*, 2826–2827.
- (12) Boldyrev, A. I.; Von Niessen, W. *Chem. Phys.* **1991**, *155*, 71–78.
- (13) Boldyrev, A. I.; Simons, J. J. *Chem. Phys.* **1993**, *99*, 4628–4637.
- (14) Gutsev, G. L.; Jena, P.; Bartlett, R. J. *Chem. Phys. Lett.* **1998**, *292*, 289–294.
- (15) Wang, X. B.; Ding, C. F.; Wang, L. S.; Boldyrev, A. I.; Simons, J. *J. Chem. Phys.* **1999**, *110*, 4763–4771.
- (16) Anusiewicz, I.; Skurski, P. *Chem. Phys. Lett.* **2002**, *358*, 426–434.
- (17) Anusiewicz, I.; Sobczyk, M.; Dabkowska, I.; Skurski, P. *Chem. Phys.* **2003**, *291*, 171–180.
- (18) Alexandrova, A. N.; Boldyrev, A. I.; Fu, Y. J.; Yang, X.; Wang, X.-B.; Wang, L.-S. *J. Chem. Phys.* **2004**, *121*, 5709–5719.
- (19) Elliot, B. M.; Koyle, E.; Boldyrev, A. I.; Wang, X.-B.; Wang, L.-S. *J. Phys. Chem. A* **2005**, *109*, 11560–11567.
- (20) Anusiewicz, I.; Skurski, P. *Chem. Phys. Lett.* **2007**, *440*, 41–44.
- (21) Anusiewicz, I. *Aust. J. Chem.* **2008**, *61*, 712–717.
- (22) Koirala, P.; Willis, M.; Kiran, B.; Kandalam, A. K.; Jena, P. *J. Phys. Chem. C* **2010**, *114*, 16018–16024.
- (23) Ko, Y. J.; Wang, H.; Pradhan, K.; Koirala, P.; Kandalam, A. K.; Bowen, K. H.; Jena, P. *J. Chem. Phys.* **2011**, *138*, 244312–244317.
- (24) Gutsev, G. L.; Rao, B. K.; Jena, P.; Wang, X. B.; Wang, L. S. *Chem. Phys. Lett.* **1999**, *312*, 598–605.
- (25) Gutsev, G. L.; Jena, P.; Zhai, H. J.; Wang, L. S. *J. Chem. Phys.* **2001**, *115*, 7935–7944.
- (26) Yang, X.; Wang, X. B.; Wang, L. S.; Niu, S.; Ichiye, T. *J. Chem. Phys.* **2003**, *119*, 8311–8320.
- (27) Sobczyk, M.; Sawicka, A.; Skurski, P. *Eur. J. Inorg. Chem.* **2003**, *20*, 3790–3797.
- (28) Yang, J.; Wang, X. B.; Xing, X. P.; Wang, L. S. *J. Chem. Phys.* **2008**, *128*, 201102–201105.
- (29) Pradhan, K.; Gutsev, G. L.; Jena, P. *J. Chem. Phys.* **2010**, *133*, 144301–144308.
- (30) Wu, M. M.; Wang, H.; Ko, Y. J.; Wang, Q.; Sun, Q.; Kiran, B.; Kandalam, A. K.; Bowen, K. H.; Jena, P. *Angew. Chem., Int. Ed.* **2011**, *50*, 2568–2572.
- (31) Pradhan, K.; Gutsev, G. L.; Weatherford, C. A.; Jena, P. *J. Chem. Phys.* **2011**, *134*, 234311–234318.
- (32) Zhai, H. J.; Wang, L. M.; Li, S. D.; Wang, L. S. *J. Phys. Chem. A* **2007**, *111*, 1030–1035.
- (33) Pathak, B.; Samanta, D.; Ahuja, R.; Jena, P. *ChemPhysChem* **2011**, *12*, 2423–2428.
- (34) Samanta, D.; Wu, M. M.; Jena, P. *Inorg. Chem.* **2011**, *50*, 8918–8925.
- (35) Willis, M.; Götz, M.; Kandalam, A. K.; Ganteför, G. F.; Jena, P. *Angew. Chem., Int. Ed.* **2010**, *49*, 8966–8970.
- (36) Feng, Y.; Xu, H. G.; Zheng, W.; Zhao, H.; Kandalam, A. K.; Jena, P. *J. Chem. Phys.* **2011**, *134*, 094309–094316.
- (37) Pradhan, K.; Jena, P. *J. Chem. Phys.* **2011**, *135*, 144305–144310.
- (38) Gutsev, G. L.; Weatherford, C. A.; Johnson, L. E.; Jena, P. *J. Comput. Chem.* **2012**, *33*, 416–424.
- (39) Paduani, C.; Jena, P. *J. Phys. Chem. A* **2012**, *116*, 1469–1474.
- (40) Becke, A. D. *J. Chem. Phys.* **1993**, *98*, 5648–5652.
- (41) Lee, C.; Yang, W.; Parr, R. G. *Phys. Rev. B* **1988**, *37*, 785–789.
- (42) Frisch, M. J.; Trucks, G. W.; Schlegel, H. B.; Scuseria, G. E.; Robb, M. A.; Cheeseman, J. R.; Montgomery, J. A., Jr.; Vreven, T.; Kudin, K. N.; Burant, J. C.; et al. *Gaussian 03*, Revision C.02; Gaussian, Inc.: Wallingford, CT, 2004.
- (43) Feng, Y.; Xu, H. G.; Zhang, Z. G.; Gao, Z.; Zheng, W. *J. Chem. Phys.* **2010**, *132*, 074308–074313.